Metastable reverse-phase droplets within ordered phases: Renormalization-group calculation of field and temperature dependence of limiting size

Ege Eren[1] and A. Nihat Berker[2,3]
[1]*Department of Electrical Engineering, Boğaziçi University, Bebek, Istanbul 34342, Turkey*
[2]*Faculty of Engineering and Natural Sciences, Kadir Has University, Cibali, Istanbul 34083, Turkey*
[3]*Department of Physics, Massachusetts Institute of Technology, Cambridge, Massachusetts 02139, USA*

(Received 26 February 2020; accepted 6 April 2020; published 23 April 2020)

Metastable reverse-phase droplets are calculated by renormalization-group theory by evaluating the magnetization of a droplet under magnetic field, matching the boundary condition with the reverse phase and noting whether the reverse-phase magnetization sustains. The maximal metastable droplet size and the discontinuity across the droplet boundary are thus calculated as a function of temperature and magnetic field for the Ising model in three dimensions. The method also yields hysteresis loops for finite systems, as function of temperature and system size.

DOI: 10.1103/PhysRevE.101.042127

I. INTRODUCTION: CALCULATED SUSTAINABILITY OF METASTABLE DROPLETS

After outstanding success in the calculation of critical exponents and in understanding the mechanism underlying the universality of critical exponents, renormalization-group theory has been equally successfully applied to global nonuniversal properties at and away from critical points, such as entire thermodynamic functions, discontinuities at first-order phase transitions, and entire multicritical phase diagrams, e.g., leading all the way to global spin-glass phase diagrams in the variables of temperature, bond concentration, spatial dimensionality d, and the continuous variation of chaos and its Lyapunov exponent inside spin-glass phases [1,2]. Such wide application has not yet been reached in nonequilibrium systems. On the other hand, renormalization-group calculations have been applied to finite-sized systems [3]. As explained below, these calculations can be used to obtain the properties of nonequilibrium metastable droplets inside ordered phases and the hysteresis loops of systems partitioned into domains. In addition to the metastable applications mentioned above, our calculations are applicable to paint cratering due to surface defects [4].

Nonequilibrium studies away from the critical point have been on the droplet formation of the equilibrium phase, inside the nonequilibrium metastable phase (after a deep quench). For the much studied Classical Nucleation Theory, see Refs. [5–11]. We tackle here the converse problem, namely, the existence of metastable droplets of the nonequilibrium phase, inside the equilibrium phase. We find that such droplets exist and are clearly delimited by size, magnetic field, and temperature, the last two being a measure of the thermodynamic distance to the first-order phase boundary where the nonequilibrium phase becomes a coexisting phase.

II. BOUNDARY-CONDITIONED FINITE-SYSTEM CALCULATION FOR THE PRESENCE OF A METASTABLE DROPLET

Finite-system renormalization-group calculation [3] can readily be adapted to metastable droplet viability. Such a droplet is a finite region of the opposite thermodynamic phase persisting inside the equilibrium phase. Even as a metastable region, a droplet can exist up to a certain (critical) size, depending on how far away, in the thermodynamic external (applied) variables, the system is from the boundary in thermodynamic space where the phase of the droplet becomes stable. The farther away, the smaller the maximal droplet size, up to a certain limit, beyond which metastable droplets do not exist. This critical droplet size and this limit of metastable droplet existence are obtained, based on a microscopic statistical mechanical (renormalization-group) calculation, in our current work.

We illustrate with the Ising model, defined by the Hamiltonian

$$-\beta\mathcal{H} = J\sum_{\langle ij\rangle} s_i s_j + H\sum_i s_i, \tag{1}$$

where $\beta = 1/kT$, at each site i of the lattice the spin $s_i = \pm 1$, and $\langle ij\rangle$ denotes summation over all nearest-neighbor site pairs. The bond is ferromagnetic, $J > 0$, and J^{-1} is thus the temperature variable. In three spatial dimensions ($d = 3$), this system has the phase diagram shown in Fig. 1. The equilibrium phases are indicated. As is well known, for $T < T_C$ on the $H = 0$ line, there is a first-order phase transition between the down-magnetized phase with $M = \langle s_i\rangle < 0$ and the up-magnetized phase with $M > 0$. At the position in the phase diagram marked by $\times$, where $H > 0$, the equilibrium phase is the up-magnetized phase with $M > 0$, but metastable droplets of the down-magnetized phase with $M < 0$ can exist, depending on the value of H, which gives the thermodynamic-variable distance from the phase boundary.

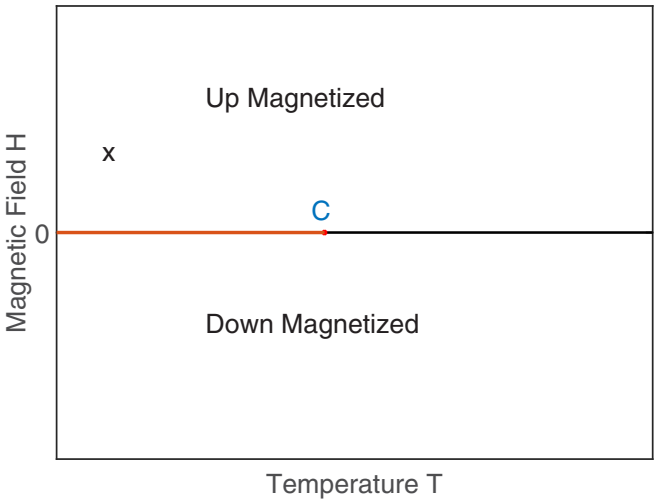

FIG. 1. Phase diagram of the ferromagnetic Ising model for $d > 1$. The equilibrium phases are indicated. For $T < T_C$ on the $H = 0$ line, there is a first-order phase transition between the down-magnetized phase and the up-magnetized phase. At the position in the phase diagram marked with the $\times$, the equilibrium phase is the up-magnetized phase, but metastable droplets of the down-magnetized phase can exist, depending on the thermodynamic-variable distance from the phase boundary.

The basis of our method is as follows: Renormalization-group theory enables us to calculate the thermodynamic properties, including magnetization M of finite and infinite systems. Thus, we calculate the magnetization inside a droplet of size L at position $\times$ on Fig. 1, that is under the system-wide applicable value of $H > 0$. As illustrated in Fig. 2, we

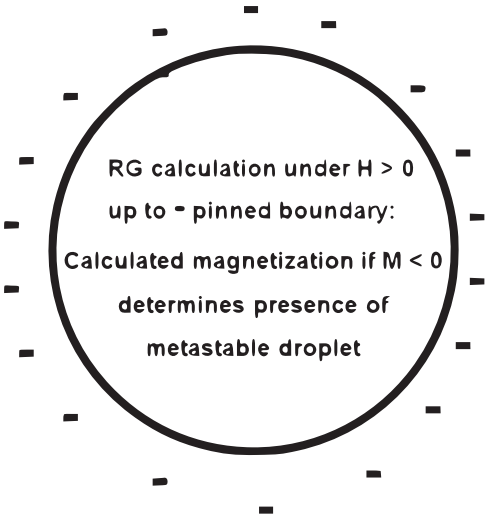

FIG. 2. The magnetization is calculated inside a droplet of size L at position $\times$ in Fig. 1, which is under the system-wide applicable value of $H > 0$, matching with the boundary condition of down-pinned, $s_i = -1$ spins. This boundary represents the outermost layer of the would-be droplet. If this calculation gives $M < 0$ inside the droplet, the droplet exists. Note that our calculation is for a cubic shape, under the Migdal-Kadanof approximation, not the spherical object shown in this figure that pedagogically explains our method.

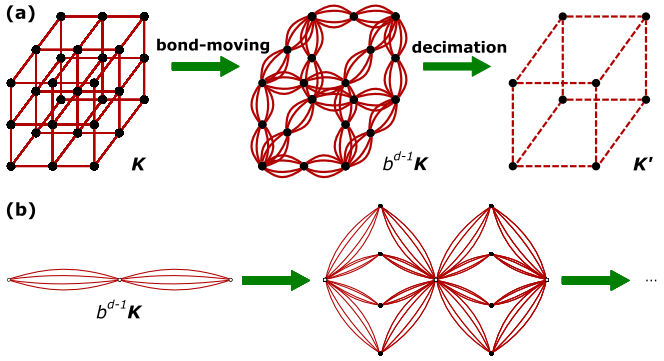

FIG. 3. (a) Migdal-Kadanoff approximate renormalization-group transformation for the $d = 3$ cubic lattice with the length-rescaling factor of $b = 2$. (b) Construction of the $d = 3, b = 2$ hierarchical lattice for which the Migdal-Kadanoff recursion relations are exact. The renormalization-group solution of a hierarchical lattice proceeds in the opposite direction of its construction.

match with the boundary condition of down-pinned, $s_i = -1$ spins. This boundary represents the outermost layer of the would-be droplet. If this calculation gives $M < 0$ inside the droplet, the droplet exists. If, in this calculation, the applied field $H > 0$ overcomes the down-pinned boundary condition $s_i = -1$ and $M > 0$, then the droplet of size L does not exist. Since under renormalization-group transformation, the value of the magnetic field increases, there is clearly a maximal value $L_C(H)$, where H refers to the initial (unrenormalized) magnetic fields, to the metastable droplet size.

III. RENORMALIZATION-GROUP CALCULATION

For our calculation, we use the Migdal-Kadanoff approximation, which, as shown in Fig. 3(a), consists in bond moving followed by decimation [12,13]. This much used approximation gives, for the first renormalization-group transformation, the recursion relations

$$K' = K'(J, H),\ h' = h'(J, H),\ G' = G'(J, H), \qquad (2)$$

where the primes refer to the renormalized quantities and G is the additive constant in the Hamiltonian automatically generated by the renormalization-group transformation:

$$-\beta\mathcal{H} = \sum_{\langle ij\rangle}[Ks_is_j + h(s_i + s_j) + G]. \qquad (3)$$

In the latter equation, the magnetic field term is expressed in the form that it takes after the first renormalization-group transformation. After the first renormalization-group transformation, the form of the Hamiltonian in Eq. (3) is conserved and the recursion relations have the form

$$K' = K'(K, h),\ h' = h'(K, h),\ G' = b^dG + g(K, h). \qquad (4)$$

The recursion relations thus obtained from the Migdal-Kadanoff approximation are exactly applicable to the exact solution of the hierarchical lattice shown in Fig. 3(b) [3,14,15]. Thus, a "physically realizable," therefore robust approximation is used. Physically realizable approximations have been used in polymers [16,17], disordered alloys [18],

and turbulence [19]. Recent works using exactly soluble hierarchical lattices are found in Refs. [20–25].

Sites at different levels of a hierarchical lattice have different coordination numbers. For example, on the right side of Fig. 3(b), two different levels are seen for the inner sites, with coordination numbers $q = 8$ and 16. In our calculation, the magnetic field in Eq. (1) is applied to sites in the lowest level of the hierarchy, which are the least coordinated ($q = 8$) and most numerous, comprising $1 - b^{-d} = 7/8$ of all the sites.

In the first renormalization-group transformation, going from Eq. (1) to Eq. (3) with a scale change, the thermodynamic densities are related by

$$\mathbf{M} = b^{-d}\,\mathbf{m}\cdot\mathbf{U}, \tag{5}$$

where the densities $\mathbf{M} \equiv [1, \langle s_i s_j\rangle, \langle s_i\rangle]$ and $\mathbf{m} \equiv [1, \langle s_i s_j\rangle, \langle (s_i + s_j)\rangle]$ respectively refer to Eqs. (1) and (3). The matrix is $\mathbf{U} = \partial\mathbf{k}/\partial\mathbf{K}$ with $\mathbf{k} \equiv [1, K, h]$ and $\mathbf{K} \equiv [1, J, b^{-d}H]$. The factor b^{-d} in the last vector accounts for the fact that there are as many unrenormalized fields H (applied only to the lowest level of the hierarchy) as renormalized bonds K.

In the subsequent renormalization-group transformations, the thermodynamic densities obey the recursion relation

$$\mathbf{m} = b^{-d}\mathbf{m}'\cdot\mathbf{T}, \tag{6}$$

where the densities $\mathbf{m} \equiv [1, \langle s_i s_j\rangle, \langle (s_i + s_j)\rangle]$ are conjugate to the fields $\mathbf{k} \equiv [1, K, h]$ and the recursion matrix is $\mathbf{T} = \partial\mathbf{k}'/\partial\mathbf{k}$. The densities are calculated by iterating Eq. (6) until the boundary is reached and applying the boundary condition in the right side of Eq. (6).

The calculation yields the phase diagram in Fig. 1, with the critical temperature $J^{-1} = 15.3$, which sets the temperature scale.

IV. RESULTS: CALCULATED METASTABLE DROPLET SIZE THRESHOLDS

Magnetizations, calculated as described above, inside a would-be droplet of negative magnetization immersed in the positive magnetization phase, as a function of size, are shown in Fig. 4. Results for different magnetic fields H are shown, at temperature $J^{-1} = 5$. When the magnetization calculated inside the droplet is negative, the droplet-boundary match is self-consistent and the droplet does occur. It is seen in Fig. 4 that this droplet occurrence terminates, with a discontinuity in the calculated magnetization, at a threshold size L_C. Here $L = b^n$ is the linear dimension of the droplet, where n is the number of renormalization-group transformations needed for the many-times renormalized spin nearest separation to span the droplet.

Threshold sizes L_C, as a function of magnetic field H, are shown in Fig. 5, at temperature $J^{-1} = 5$. The threshold droplet size L_C goes to infinity as $L_C \sim H^{-0.94}$ as the system approaches the phase transition at $H = 0$. Conversely, L_C goes to zero as the system moves away from the phase transition. Metastable droplets do not occur for $H > H_{\max}(J)$, which is seen to be $H_{\max} = 1.60$ for temperature $T = J^{-1} = 5$. The inset gives $H_{\max}$ as a function of temperature. $H_{\max}$ diverges as $H_{\max} \sim T^{-1.05}$ as zero temperature is approached. At a higher temperature, there is a crossover to $H_{\max} \sim T^{-1.84}$, as seen on the left side of $T \simeq 1$ in the inset. In Fig. 5 the discreteness of the droplet size values is due to the discrete nature of the (multiplicative) length rescaling factor $b = 2$ of the renormalization-group transformation.

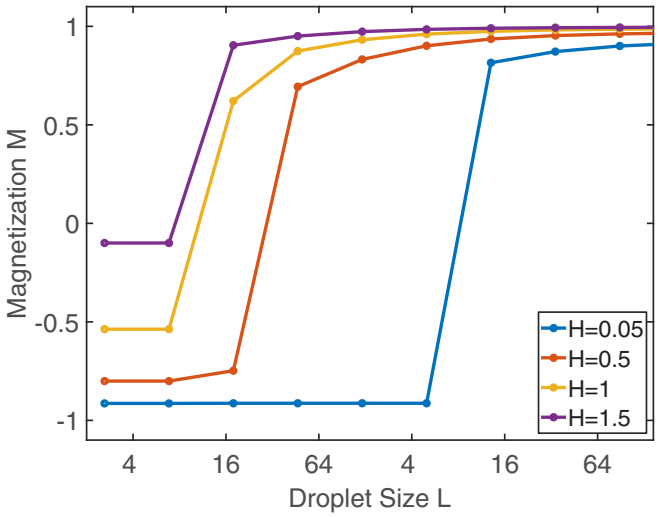

FIG. 4. Magnetization inside a would-be droplet of negative magnetization immersed in the positive magnetization phase, as a function of droplet size. Results for different magnetic fields H are shown, from left to right for $H = 0.05, 0.5, 1, 1.5$, at temperature $J^{-1} = 5$. When the magnetization calculated inside the droplet is positive, the droplet does not occur.

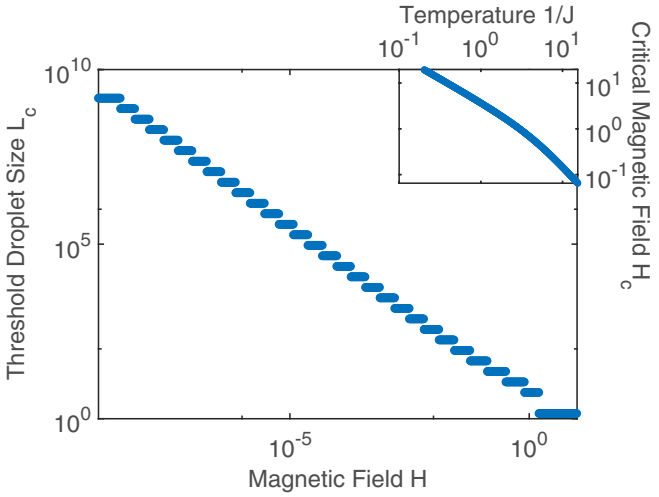

FIG. 5. Threshold sizes L_C as a function of magnetic field H, at temperature $J^{-1} = 5$. The threshold droplet size L_C goes to infinity as $L_C \sim H^{-0.94}$ as the system approaches the phase transition at $H = 0$. Conversely, L_C goes to zero as the systems moves away from the phase transition. Metastable droplets do not occur for $H > H_{\max}(J)$, which is seen to be $H_{\max} = 1.60$ for temperature $T = J^{-1} = 5$. The inset gives $H_{\max}$ as a function of temperature. $H_{\max}$ diverges as $H_{\max} \sim T^{-1.05}$ as zero temperature is approached. At a higher temperature, there is a crossover to $H_{\max} \sim T^{-1.84}$, as seen on the left side of $T \simeq 1$ in the inset.

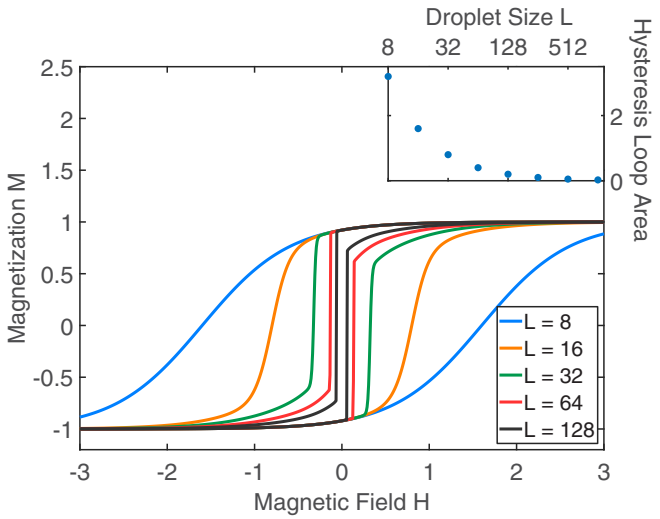

FIG. 6. Hysteresis loops at temperature $J^{-1} = 5$, for differently sized systems $L = 8, 16, 32, 64, 128$ from the sides to the middle. The loops get narrower as the system size grows, leading to a single discontinuity of the first-order phase transition of the infinite (thermodynamic limit) system. The inset shows the hysteresis loop area as a function of system size. A maximum loop area is reached when extrapolated to vanishing system size.

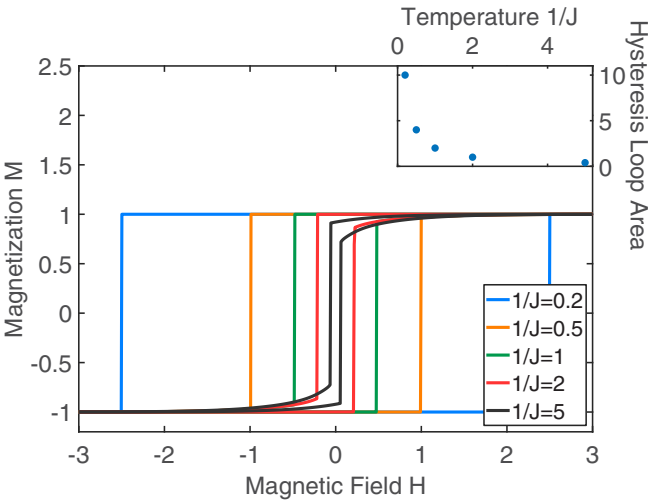

FIG. 7. Hysteresis loops at system size $L = 64$, for different temperatures $J^{-1} = 0.2, 0.5, 1, 2, 54$ from the sides to the middle. The loops get narrower as temperature increases. The inset shows the loop area as a function of temperature. The loop area diverges as zero temperature is approached.

V. RESULTS: CALCULATED HYSTERESIS LOOPS

Our current calculation can also readily be adapted to a hysteresis loop calculation. Hysteresis loops occur in systems composed of finite microdomains. As the magnetization measurements or calculations are made, the system carries a memory of the previous measurement or calculation. In the present case, this is accomplished by keeping down-pinned boundary spins as the system is scanned in the increasing H direction and conversely up-pinned boundary spins as the system is scanned in the decreasing H direction.

Thus, hysteresis loops at temperature $J^{-1} = 5$, for differently sized systems, are shown in Fig. 6. The loops get narrower as the system size grows, leading to a single discontinuity of the first-order phase transition of the infinite (thermodynamic limit) system. The inset shows the hysteresis loop area as a function of system size. A maximum loop area is reached when extrapolated to vanishing system size.

Hysteresis loops at system size $L = 64$, for different temperatures, are shown in Fig. 7. The loops get narrower as temperature increases, as the spin-spin correlations and specifically the correlations to the "memory" spins (in this case the boundary spins) decrease. The inset shows the loop area as a function of temperature. The loop area diverges as zero temperature is approached.

VI. CONCLUSION

We have calculated metastable droplets inside a stable thermodynamic phase, using renormalization-group theory. We find the droplet existence is clearly delimited by droplet size and thermodynamic distance to the stability of the phase inside the droplet. The method was also adapted to hysteresis loop calculation, yielding loop areas as a function of domain size and temperature.

We note that the inside bulk of the metastable droplet in our study increases the free energy with respect to the thermodynamically stable phase, as does the boundary between the metastable droplet and the stable phase. The phenomenological explanation for the occurrence of the metastable droplet is that there exists a free energy barrier to reverting this droplet. With increasing magnetic field, the free energy of the bulk of the droplet increases, reaching, together with the boundary free energy, the level of the free energy barrier, thus turning the barrier into a shoulder and causing the droplet to revert to the stable phase. Finally, a Monte Carlo calculation to check our results would be an interesting called-for study.

ACKNOWLEDGMENTS

A.N.B. thanks Prof. David Turnbull for encouragement of this work, some time ago. Support by the Academy of Sciences of Turkey (TÜBA) is gratefully acknowledged.

[1] E. Ilker and A. N. Berker, Phys. Rev. E **89**, 042139 (2014).
[2] B. Atalay and A. N. Berker, Phys. Rev. E **97**, 052102 (2018).
[3] A. N. Berker and S. Ostlund, J. Phys. C **12**, 4961 (1979).
[4] E. Nowak, J. M. Deutch, and A. N. Berker, J. Chem. Phys. **78**, 529 (1983).
[5] R. Becker and W. Döring, Ann. Phys. **416**, 719 (1935).
[6] J. S. Langer, Ann. Phys. (NY) **41**, 108 (1967); Phys. Rev. Lett. **21**, 973 (1968); Ann. Phys. (NY) **54**, 258 (1969).
[7] S. Ryu and W. Cai, Phys. Rev. E **82**, 011603 (2010).
[8] D. Stauffer, A. Coniglio, and D. W. Heermann, Phys. Rev. Lett. **49**, 1299 (1982).

[9] J. D. Gunton, M. San Miguel, and P. S. Sahni, The dynamics of first-order phase transitions, in *Phase Transitions and Critical Phenomena*, Vol. 8, edited by C. Domb and J. L. Lebowitz (Academic, New York, 1983), pp. 269–446.
[10] W. Klein and C. Unger, Phys. Rev. B **28**, 445 (1983).
[11] L. Monette, W. Klein, M. Zuckermann, A. Khadir, and R. Harris, Phys. Rev. B **38**, 11607 (1988).
[12] A. A. Migdal, Zh. Eksp. Teor. Fiz. **69**, 1457 (1975) [Sov. Phys. JETP **42**, 743 (1976)].
[13] L. P. Kadanoff, Ann. Phys. (NY) **100**, 359 (1976).
[14] R. B. Griffiths and M. Kaufman, Phys. Rev. B **26**, 5022 (1982).
[15] M. Kaufman and R. B. Griffiths, Phys. Rev. B **30**, 244 (1984).
[16] P. J. Flory, *Principles of Polymer Chemistry* (Cornell University Press, Ithaca, NY, 1986).
[17] M. Kaufman, Entropy **20**, 501 (2018).
[18] P. Lloyd and J. Oglesby, J. Phys. C: Solid State Phys. **9**, 4383 (1976).
[19] R. H. Kraichnan, J. Math. Phys. **2**, 124 (1961).
[20] C. Monthius, J. Stat. Mech.: Theory Exp. (2020) 013301.
[21] O. S. Sarıyer, Philos. Mag. **99**, 1787 (2018).
[22] P. A. Ruiz, Commun. Math. Phys. **364**, 1305 (2018).
[23] M. J. G. Rocha-Neto, G. Camelo-Neto, E. Nogueira, Jr., and S. Coutinho, Physica A **494**, 559 (2018).
[24] F. Ma, J. Su, Y. X. Hao, B. Yao, and G. G. Yan, Physica A **492**, 1194 (2018).
[25] S. Boettcher and S. Li, Phys. Rev. A **97**, 012309 (2018).